



## Development and evaluation of a mobile app for bone mineral densitometry in dry canine bones

Desenvolvimento e avaliação de aplicativo móvel para determinação da densidade mineral em ossos secos de cães

Thiago André Carreo Costa<sup>1\*</sup>, Adriana Castro de Jesus<sup>1</sup>, Thiago Borges de Oliveira<sup>1</sup>, Alexandre Redson Soares da Silva<sup>2</sup>, Cássio Aparecido Pereira Fontana<sup>1</sup>, Valcinir Aloísio Scalla Vulcani<sup>1</sup>

1 Universidade Federal de Jataí (UFJ), Jataí, Goiás, Brazil. 

2 Universidade Federal do Vale do São Francisco (UFVFSF), Petrolina, Pernambuco, Brazil. 

\*corresponding author: thiagocarreo@ufj.edu.br

Received: August 08, 2024. Accepted: November 18, 2024. Published: February 14, 2025. Editor: Luiz Augusto B. Brito

**Abstract:** Annually, approximately 9 million osteoporotic fractures are diagnosed worldwide. As osteoporosis is a condition classified as a public health issue—often asymptomatic and, to some extent, neglected—early diagnosis of reduced bone mineral density remains a significant challenge. In this study, the Pearson correlation coefficient was employed to compare the results of radiographic bone densitometry (RBD) using a densitometric reference based on a penetrometer manufactured from aluminum alloy 6063 ABNT and a mobile application specifically developed to perform RBD measurements, with results obtained through dual-energy X-ray absorptiometry (DXA). The analysis was conducted on dry bones (ultradistal portions of radii and femoral necks) from healthy dogs. The results for the ultradistal portion of the radius obtained via the mobile application demonstrated good correlation with DXA ( $R=0.7$ ), while the femoral neck showed very good correlation ( $R=0.8$ ). It was concluded that the mobile application analyzed in this study may, in the near future, become an important tool for the effective assessment of bone mineral density.

**Key-words:** bone mineral densitometry; innovation; mobile apps; public health.

**Resumo:** Sabe-se que, anualmente, são diagnosticadas cerca de 9 milhões de fraturas osteoporóticas no mundo e, por se tratar de uma doença considerada um problema de saúde pública, assintomática e, até certo ponto negligenciada, o diagnóstico precoce da diminuição da densidade mineral óssea ainda constitui um desafio. Neste trabalho, utilizando o coeficiente de correlação de Pearson, comparou-se os resultados da densitometria óssea radiográfica (DORX) obtidas utilizando como referencial densitométrico um penetômetro confeccionado em liga de alumínio 6063 ABNT e um aplicativo móvel especialmente desenvolvido para realizar a aferição, com resultados obtidos pela absorptometria de raios-X de dupla energia (DXA). Foram analisados ossos secos (porções ultradistais de rádios e colos femorais) de cães sadios. Os resultados da análise da porção ultradistal do rádio obtidos por meio do aplicativo mostraram correlação boa quando comparados com a DXA ( $R=0,7$ ) e, para o colo femoral, correlação muito boa ( $R=0,8$ ). Concluiu-se que a aplicação móvel analisada neste estudo pode, em um futuro próximo, se tornar uma ferramenta importante para análise densidade mineral óssea de maneira eficaz.

**Palavras-chave:** densitometria; inovação; aplicativo; osso.



## 1. Introduction

With approximately 8.9 million osteoporotic fractures occurring annually, osteoporosis has become a significant global public health concern <sup>(1)</sup>. Often referred to as a “silent epidemic” due to its asymptomatic nature until fractures occur <sup>(2)</sup>, osteoporosis has historically received less attention from governments and public health advocates compared to other chronic non-communicable diseases <sup>(3,4)</sup>. Since 1987, dual-energy X-ray absorptiometry (DXA) has been widely regarded as the gold standard for assessing bone mineral density (BMD) <sup>(4-7)</sup>. This technique can be applied to peripheral bones, such as the calcaneus, distal radius, metacarpals, and phalanges, as well as to the vertebrae and femoral neck, enabling the prediction of fracture risk <sup>(8,9)</sup>. Although DXA is the gold standard for diagnosing osteoporosis, a study by the International Osteoporosis Foundation revealed significant disparities in its availability. Countries such as Australia, Hong Kong, Japan, New Zealand, and Singapore have up to 24 DXA machines per million inhabitants, whereas nations such as China, India, Indonesia, Pakistan, Philippines, Sri Lanka, and Vietnam have fewer than one per million <sup>(10)</sup>. In Latin America, Brazil and Chile lead with 10 DXA machines per million inhabitants, while other countries range from 0.9 to 6.7 per million <sup>(11)</sup>.

Only one in four patients diagnosed with fragility fractures has received prophylactic treatment <sup>(12)</sup>, underscoring the ongoing challenge of osteoporosis as a public health issue. Less than 20% of patients with fragility fractures are treated to reduce the risk of subsequent fractures <sup>(13-15)</sup>. A study across four Latin American countries (Argentina, Brazil, Colombia, and Mexico), representing a combined population of approximately 500 million, reported 850,000 fracture cases in 2018, resulting in a financial impact exceeding one billion USD <sup>(12)</sup>.

These findings are particularly significant in Central and South America where access to densitometric data is limited or prohibitively expensive. A substantial proportion of the population lives below the poverty line, and preventive health measures targeting osteoporosis and musculoskeletal disorders are not a priority <sup>(16,17)</sup>. To address these challenges, this study evaluated the precision of a mobile application developed at the Federal University of Jataí (UFJ) to determine BMD using simple radiographic examinations and an aluminum densitometric reference.

## 2. Material and methods

Dry bones (anatomical specimens) were obtained from the Veterinary Anatomy Collection of the Federal University of Jataí (UFJ). The sample comprised five femurs and six radii of adult male and female dogs without a history of metabolic or musculoskeletal disorders. Two techniques were employed to determine the BMD of each specimen: Dual-energy X-ray absorptiometry (DXA) and Optical densitometry in radiographic images (DORX) using a reference phantom made from a specific aluminum alloy (6063 ABNT) comprising Al-Mg-Si <sup>(18,19)</sup>. The composition included 98.75% aluminum, 0.54% magnesium, 0.47% silicon, and 0.24% other elements, as per international standards. The phantom measured 10 × 55

mm, with 11 steps varying in height from 0.5 to 9.0 mm, and was positioned adjacent to, but not in contact with, the bones (Figure 1).



**Figure 1.** Example of the radiographic image of the femur (A), the 6063 ABNT aluminum phantom with 11 steps (B), and the radius (C) obtained using the Lunar DPX-NT Series 76KV X-Ray Tube House Assembly from GE Medical Systems.

For DXA, a Lunar DPX-NT Series 76KV X-Ray Tube House Assembly (GE Medical Systems) was used to target the femoral neck and ultradistal radius (UD) as regions of interest (ROI). The methodology proposed by Vulcano *et al.* (2008) <sup>(20)</sup> was followed to examine the same anatomical regions as in DXA. Radiographs were acquired using a Poskom<sup>®</sup> Vet 20BT X-ray device and a Kylumax<sup>®</sup> KLX-1417 digital X-ray scanner (46 × 34.8 cm, 16-bit resolution, 3.6 line pairs/mm). Exposure techniques were 70 kV/1.2 mAs for the femoral neck and 65 kV/1.2 mAs for the UD radius. The 11-step aluminum phantom was placed beside the bones for densitometric reference measurements.

Radiographic data were exported as JPEG files were analyzed using a custom-built mobile application (APP) developed in Android Studio with Java support and the OpenCV library. The analysis involved the following three steps: 1. Opening the radiographic image in the APP, 2. Manual selection of the ROI by the user, followed by automatic detection of the phantom, and 3. Calculating the BMD of the ROI using the average grayscale values for each phantom step, which were correlated with the aluminum thickness in millimeters (mmAl).

The APP processes grayscale values ranging from 0 (absolute black) to 255 (absolute white), correlating the radiographic density to the pixel intensity. The algorithm calculates the BMD values for the ROI based on linear regression between the grayscale values of the phantom and the aluminum thickness. Pearson's correlation coefficient ( $r$ ) was calculated to evaluate the correlation between APP and DXA results. Correlation was classified as follows: no correlation ( $r = 0$ ), very poor ( $0 < r \leq 0.2$ ), poor ( $0.2 < r \leq 0.4$ ), moderate ( $0.4 < r \leq 0.6$ ), good ( $0.6 < r \leq 0.8$ ), very good ( $0.8 < r < 1$ ), and perfect ( $r = 1$ ) <sup>(21, 22)</sup>. Statistical analyses and regression equations were generated using Microsoft Excel<sup>®</sup> 2019.

### 3. Results

Both DXA and DORX successfully determined the BMD of all analyzed bones, despite the examinations being performed on anatomical specimens. The results obtained through the DXA and DORX examinations are presented in Table 1 (absolute values and mean values  $\pm$  standard deviation [SD]).

**Table 1.** BMD values of the femoral neck and ultradistal radius (UD) of dogs obtained using dual-energy X-ray absorptiometry (DXA) in  $\text{g}/\text{cm}^2$ , along with the values from three repetitions and mean  $\pm$  standard deviation (in  $\text{mmAl}$ ) from simple radiographic examinations using an aluminum densitometric reference.

	APP Result 1 (mmAl)	APP Result 2 (mmAl)	APP Result 3 (mmAl)	Mean $\pm$ SD (mmAl)	DXA Result ( $\text{g}/\text{cm}^2$ )
Femoral Neck (1)	4.01	4.00	4.00	4.00 $\pm$ 0.006	0.715
Femoral Neck (2)	3.92	3.91	3.91	3.91 $\pm$ 0.006	0.680
Femoral Neck (3)	4.51	4.49	4.49	4.50 $\pm$ 0.012	0.718
Femoral Neck (4)	4.71	4.71	4.72	4.71 $\pm$ 0.006	0.866
Femoral Neck (5)	4.16	4.15	4.17	4.16 $\pm$ 0.010	0.648
Ultradistal Radius (1)	3.06	3.06	3.05	3.06 $\pm$ 0.006	0.567
Ultradistal Radius (2)	3.49	3.52	3.50	3.50 $\pm$ 0.015	0.647
Ultradistal Radius (3)	3.34	3.32	3.33	3.33 $\pm$ 0.010	0.552
Ultradistal Radius (4)	3.31	3.30	3.30	3.30 $\pm$ 0.006	0.586
Ultradistal Radius (5)	2.94	2.95	2.95	2.95 $\pm$ 0.006	0.513
Ultradistal Radius (6)	2.85	2.85	2.87	2.86 $\pm$ 0.012	0.576

Correlation equations were established between the two methods based on the densitometric values obtained from the bones. For the femoral neck, the equation  $y = 7.2756x^2 - 7.9832x + 6.1792$  was generated, with a coefficient of determination of  $R^2 = 0.618$ . For the ultradistal radius (UD), the equation  $y = 20.135x^2 - 19.722x + 7.8214$  was obtained, with a coefficient of determination of  $R^2 = 0.458$  (Figure 2). The correlation coefficients were subsequently calculated, yielding  $R = 0.8$  for the femoral neck and  $R = 0.7$  for the ultradistal radius.

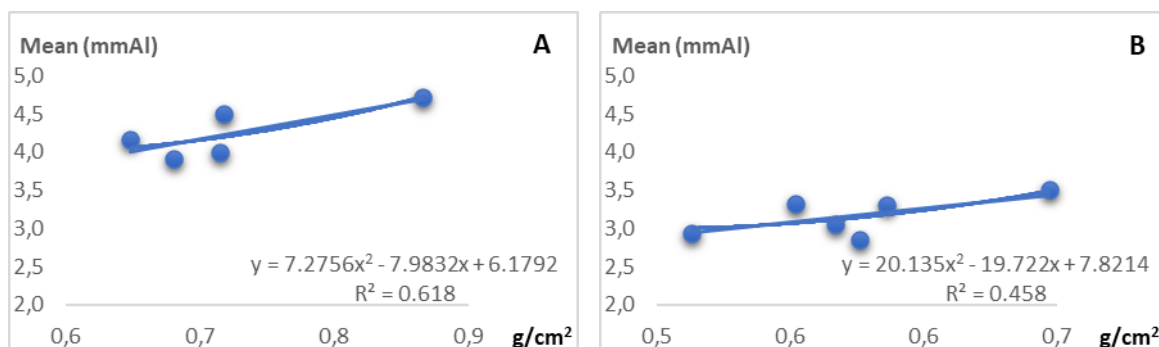


**Figure 2.** Bone densitometry values (expressed in mmAl) obtained through a mobile application using optical densitometry in radiographic images with a reference phantom made of 6063 ABNT aluminum alloy and through dual-energy X-ray absorptiometry (expressed in g/cm<sup>2</sup>) from dry canine bones sourced from the veterinary anatomy department of UFJ-GO. A, femoral neck; B, ultradistal radius (UD).

#### 4. Discussion

Osteoporosis and fragility fractures are well known to be associated with increased mortality rates <sup>(23)</sup>. This study analyzed two different ROIs: the femoral neck, recommended by the World Health Organization as the primary site for osteoporosis diagnosis <sup>(24)</sup>, and the radius, which can also be evaluated when the hip and/or lumbar spine cannot be assessed because peripheral bones are valid alternatives for diagnosing osteoporosis via densitometry <sup>(8, 25)</sup>.

This experiment can be considered relevant because with technological advancements, diagnostic equipment and tools with embedded software have gained significant attention. Many techniques have been developed to predict various pathological disorders, including image-processing algorithms for medical diagnosis. Similar to the APP developed in this study, these systems demonstrated improved precision, greater efficiency, and lower costs for osteoporosis diagnosis. Therefore, simple radiographic examinations are performed to detect osteoporosis <sup>(26, 27)</sup>.

Both methods for bone mineral density (BMD) determination in this study utilized X-ray radiation to produce two-dimensional images of three-dimensional structures. The image formation is based on the differential absorption of radiation by the analyzed tissue. Greater tissue density and thickness correspond to increased radiation absorption, resulting in pixel intensities on the sensor that form grayscale tones equivalent to the attenuation that occurs <sup>(21)</sup>. Although DORX does not account for soft tissue attenuation like DXA does, potentially giving DXA an advantage <sup>(28)</sup>, this experiment used dry bones, eliminating the possibility of DXA gaining an advantage over DORX.

In all 11 radiographs, the same aluminum phantom with 11 steps of varying heights (different thicknesses) was used, which was made of a 6063 ABNT aluminum alloy. It was observed that the thickness was directly proportional to the grayscale tone <sup>(29)</sup>. Consistent with previous studies, the coefficient of variation was employed as a commonly used method for assessing the repeatability of bone measurements, ensuring robust statistical analysis of the results <sup>(30, 31)</sup>.

In the optical densitometry of radiographic images, using an aluminum phantom as a reference, the method demonstrated that, while it is less precise in determining BMD than DXA, it can serve as a viable alternative, especially as a screening tool. This is due to its lower cost and reduced infrastructure requirements, which make it a more accessible option for patients <sup>(28)</sup>. DXA was used as the reference on the x-axis because it is the gold standard. Positive and progressive correlations were observed in both bones. The femoral neck samples showed less dispersion, as indicated by a higher correlation coefficient than the ultradistal radius (femoral neck,  $R=0.8$ ; radius, UD,  $R=0.7$ ).

In this experiment, consistent with other studies <sup>(32-34)</sup>, the correlation coefficient was considered good for the femoral neck and moderate for the UD radius, indicating satisfactory precision in analyzing anatomical specimens <sup>(35)</sup> and supporting the relative reliability of this method <sup>(36,37)</sup>. Finally, it should be noted that the method presented in this article will undergo further testing to enable routine clinical application, limiting its current evidence for fracture prediction <sup>(27)</sup>. Moreover, the correlation coefficient may have been higher if not due to user difficulties in precisely delineating the same ROI in examinations performed using different techniques <sup>(38)</sup>.

## 5. Conclusion

The very good correlation coefficient for the femoral neck assessment ( $R=0.8$ ) and the good correlation for the ultradistal radius ( $R=0.7$ ) indicate that the use of the mobile application developed for bone mineral density quantification may serve as a viable option to promote the popularization and increased accessibility of bone densitometry in the clinical evaluation of osteoporosis. Further studies are required, involving both a larger sample size and examinations performed on live animals, to enable a more robust analysis of the application's accuracy, sensitivity, and specificity.

### Conflict of interest statement

The authors declare no conflict of interest.

### Data availability statement

The complete experimental data will be made available upon request to the corresponding author. Although the mobile application is not currently available for download from app stores, it can be provided to interested researchers upon request, along with authorization for its use.

### Author contributions

Conceptualization: T. A. C. Costa. Data curation: T. A. C. Costa and A. C. de Jesus. Formal analysis: T. A. C. Costa, V. A. S. Vulcani and A. C. de Jesus. Investigation: A. C. de Jesus. Project administration: T. A. C. Costa. Software: T. B. de Oliveira. Resources: C. A. P. Fontana. Supervision: V. A. S. Vulcani. Validation: T. A. C. Costa. Writing (original draft): A. C. de Jesus. Writing (review & editing): T. A. C. Costa, A. R. S. da Silva and V. A. S. Vulcani.

### References

1. Johnell O, Kanis JA. An estimate of the worldwide prevalence and disability associated with osteoporotic fractures. *Osteoporos Int.* 2006 Dec;17(12):1726-33. <https://doi.org/10.1007/s00198-006-0172-4>

2. Hamdy RC. Osteoporosis, the deafening silent epidemic. *South Med J.* 2002 Jun;95(6):567-8. doi: <https://doi.org/10.1097/00007611-200206000-00001>. (<https://pubmed.ncbi.nlm.nih.gov/12081211/>)
3. Curtis EM, Moon RJ, Harvey NC, Cooper C. The impact of fragility fracture and approaches to osteoporosis risk assessment worldwide. *Bone.* 2017 Nov;104:29-38. <https://doi.org/10.1016/j.bone.2017.01.024>
4. Estanislau CA., Rahal, S.C., Müller, S.S., Louzada, M.J.Q., Estanislau, C.A., Araújo, F.A.P. Evaluation of femur of orchietomized guinea pigs by bone densitometry using dual-energy X-ray absorptiometry (DXA) and mechanical testing. *Vet e Zootec.* 2010 mar.; 17(1):104-112. (<https://repositorio.unesp.br/items/3468dd3f-5496-4311-a849-ea449a6a33d6>)
5. Marshall D, Johnell O, Wedel H. Meta-analysis of how well measures of bone mineral density predict occurrence of osteoporotic fractures. *BMJ.* 1996 May 18;312(7041):1254-9. <https://doi.org/10.1136/bmj.312.7041.1254>
6. Leslie WD, Crandall CJ. Population-Based Osteoporosis Primary Prevention and Screening for Quality of Care in Osteoporosis, Current Osteoporosis Reports. *Curr Osteoporos Rep.* 2019 Dec;17(6):483-490. <https://doi.org/10.1007/s11914-019-00542-w>
7. Rubin KH, Friis-Holmberg T, Hermann AP, Abrahamsen B, Brixen K. Risk assessment tools to identify women with increased risk of osteoporotic fracture: complexity or simplicity? A systematic review. *J Bone Miner Res.* 2013 Aug;28(8):1701-17. <https://doi.org/10.1002/jbmr.1956>
8. Eftekhari-Sadat B, Ghavami M, Toopchizadeh V, Ghahvechi Akbari M. Wrist bone mineral density utility in diagnosing hip osteoporosis in postmenopausal women. *Ther Adv Endocrinol Metab.* 2016 Dec;7(5-6):207-211. <https://doi.org/10.1177/2042018816658164>
9. Ilic Stojanovic O, Vuceljic M, Lazovic M, Gajic M, Radosavljevic N, Nikolic D, Andjic M, Spiroski D, Vujovic S. Bone mineral density at different sites and vertebral fractures in Serbian postmenopausal women. *Climacteric.* 2017 Feb;20(1):37-43. <https://doi.org/10.1080/13697137.2016.1253054>
10. Mithal A, Bansal B, Kyer CS, Ebeling P. The Asia-Pacific Regional Audit-Epidemiology, Costs, and Burden of Osteoporosis in India 2013: A report of International Osteoporosis Foundation. *Indian J Endocrinol Metab.* 2014 Jul;18(4):449-54. <https://doi.org/10.4103/2230-8210.137485>.
11. Harvey NC, McCloskey EV, Mitchell PJ, Dawson-Hughes B, Pierroz DD, Reginster JY, Rizzoli R, Cooper C, Kanis JA. Mind the (treatment) gap: a global perspective on current and future strategies for prevention of fragility fractures. *Osteoporos Int.* 2017 May;28(5):1507-1529. <https://doi.org/10.1007/s00198-016-3894-y>
12. Aziziyeh R, Amin M, Habib M, Garcia Perlaza J, Szafranski K, McTavish RK, Disher T, Lüdke A, Cameron C. The burden of osteoporosis in four Latin American countries: Brazil, Mexico, Colombia, and Argentina. *J Med Econ.* 2019 Jul;22(7):638-644. <https://doi.org/10.1080/13696998.2019.1590843>
13. Elliot-Gibson V, Bogoch ER, Jamal SA, Beaton DE. Practice patterns in the diagnosis and treatment of osteoporosis after a fragility fracture: a systematic review. *Osteoporos Int.* 2004 Oct;15(10):767-78. <https://doi.org/10.1007/s00198-004-1675-5>.
14. Giangregorio L, Papaioannou A, Cranney A, Zytaruk N, Adachi JD. Fragility fractures and the osteoporosis care gap: an international phenomenon. *Semin Arthritis Rheum.* 2006 Apr;35(5):293-305. <https://doi.org/10.1016/j.semarthrit.2005.11.001>.
15. Haaland DA, Cohen DR, Kennedy CC, Khalidi NA, Adachi JD, Papaioannou A. Closing the osteoporosis care gap: increased osteoporosis awareness among geriatrics and rehabilitation teams. *BMC Geriatr.* 2009 Jul 14;9:28. <https://doi.org/10.1186/1471-2318-9-28>.
16. Mautalen C, Schianchi A, Sigal D, Gianetti G, Vidan V, Bagur A, González D, Mastaglia S, Oliveri B. Prevalence of Osteoporosis in Women in Buenos Aires Based on Bone Mineral Density at the Lumbar Spine and Femur. *J Clin Densitom.* 2016 Oct;19(4):471-476. <https://doi.org/10.1016/j.jocd.2016.01.003>.
17. Pinheiro MM, Ciconelli RM, Martini LA, Ferraz MB. Clinical risk factors for osteoporotic fractures in Brazilian women and men: the Brazilian Osteoporosis Study (BRAZOS). *Osteoporos Int.* 2009 Mar;20(3):399-408. <https://doi.org/10.1007/s00198-008-0680-5>.

18. Associação Brasileira de Normas Técnicas. NBR 8117: Alumínio e suas ligas – Arames, barras, perfis e tubos extrudados - Requisitos. Rio de Janeiro, 10.p. 2011. (<https://www.normas.com.br/visualizar/abnt-nbr-nm/1122/abnt-nbr8117-aluminio-e-suas-ligas-arames-barras-perfis-e-tubos-extrudados-requisitos>)
19. Asensio-Lozano J, Suárez-Peña B, Vander Voort GF. Effect of Processing Steps on the Mechanical Properties and Surface Appearance of 6063 Aluminium Extruded Products. *Materials* (Basel). 2014 May 30;7(6):4224-4242. doi: <https://doi.org/10.3390/ma7064224>.
20. Vulcano LC, Santos FAMd, Godoy CLBd. Determinação da densidade mineral óssea da extremidade distal do rádio-ulna em gatos: correlação entre peso, sexo e idade. *Cienc Rural*. 2008;38(1):124-8. doi: <https://doi.org/10.1590/S0103-84782008000100020>
21. Lucas K, Nolte I, Galindo-Zamora V, Lerch M, Stukenborg-Colsman C, Behrens BA, et al. Comparative measurements of bone mineral density and bone contrast values in canine femora using dual-energy X-ray absorptiometry and conventional digital radiography. *BMC veterinary research*. 2017;13(1):130. <https://doi.org/10.1186/s12917-017-1047-y>
22. Robertson G, Wallace R, Simpson AHRW, Dawson SP. Preoperative measures of bone mineral density from digital wrist radiographs. *Bone Joint Res*. 2021 Dec;10(12):830-839. <https://doi.org/10.1302/2046-3758.1012.BJR-2021-0098.R1>
23. Lucas K, Nolte I, Galindo-Zamora V, Lerch M, Stukenborg-Colsman C, Behrens BA, Bouguecha A, Betancur S, Almohallami A, Wefstaedt P. Comparative measurements of bone mineral density and bone contrast values in canine femora using dual-energy X-ray absorptiometry and conventional digital radiography. *BMC Vet Res*. 2017 May 11;13(1):130. <https://doi.org/10.1186/s12917-017-1047-y>
24. Sözen T, Özişik L, Başaran NÇ. An overview and management of osteoporosis. *Eur J Rheumatol*. 2017 Mar;4(1):46-56. <https://doi.org/10.5152/eurjrheum.2016.048>.
25. Abdelmohsen AM. Comparison of Central and Peripheral Bone Mineral Density Measurements in Postmenopausal Women. *J Chiropr Med*. 2017 Sep;16(3):199-203. <https://doi.org/10.1016/j.jcm.2017.08.001>
26. Assessment of fracture risk and its application to screening for postmenopausal osteoporosis. Report of a WHO Study Group. *World Health Organ Tech Rep Ser*. 1994;843:1-129. <https://pubmed.ncbi.nlm.nih.gov/7941614/>
27. Wani IM, Arora S. Computer-aided diagnosis systems for osteoporosis detection: a comprehensive survey. *Med Biol Eng Comput*. 2020 Sep;58(9):1873-1917. <https://doi.org/10.1007/s11517-020-02171-3>
28. Sollmann N, Löffler MT, Kronthaler S, Böhm C, Dieckmeyer M, Ruschke S, Kirschke JS, Carballido-Gamio J, Karampinos DC, Krug R, Baum T. MRI-Based Quantitative Osteoporosis Imaging at the Spine and Femur. *J Magn Reson Imaging*. 2021 Jul;54(1):12-35. <https://doi.org/10.1002/jmri.27260>
29. Dendere R, Whiley SP, Douglas TS. Computed digital absorptiometry for measurement of phalangeal bone mineral mass on a slot-scanning digital radiography system. *Osteoporos Int*. 2014 Nov;25(11):2625-30. <https://doi.org/10.1007/s00198-014-2792-4>
30. Cook WD. An investigation of the radiopacity of composite restorative materials. *Aust Dent J*. 1981 Apr;26(2):105-12. <https://doi.org/10.1111/j.1834-7819.1981.tb02443.x>
31. Blake GM, Fogelman I. An update on dual-energy x-ray absorptiometry. *Semin Nucl Med*. 2010 Jan;40(1):62-73. <https://doi.org/10.1053/j.semnuclmed.2009.08.001>.
32. El Maghraoui A, Roux C. DXA scanning in clinical practice. *QJM*. 2008 Aug;101(8):605-17. <https://doi.org/10.1093/qjmed/hcn022>
33. Ravn P, Overgaard K, Huang C, Ross PD, Green D, McClung M. Comparison of bone densitometry of the phalanges, distal forearm and axial skeleton in early postmenopausal women participating in the EPIC Study. *Osteoporos Int*. 1996;6(4):308-13. <https://doi.org/10.1007/BF01623390>
34. Sotoca JM, Iñesta JM, Belmonte MA. Hand bone segmentation in radioabsorptiometry images for computerised bone mass assessment. *Comput Med Imaging Graph*. 2003 Nov-Dec;27(6):459-67. [https://doi.org/10.1016/s0895-6111\(03\)00053-3](https://doi.org/10.1016/s0895-6111(03)00053-3)

35. Yang SO, Hagiwara S, Engelke K, Dhillon MS, Guglielmi G, Bendavid EJ, Soejima O, Nelson DL, Genant HK. Radiographic absorptiometry for bone mineral measurement of the phalanges: precision and accuracy study. *Radiology*. 1994 Sep;192(3):857-9. <https://doi.org/10.1148/radiology.192.3.8058960>

36. Kastl S, Sommer T, Klein P, Hohenberger W, Engelke K. Accuracy and precision of bone mineral density and bone mineral content in excised rat humeri using fan beam dual-energy X-ray absorptiometry. *Bone*. 2002 Jan;30(1):243-6. [https://doi.org/10.1016/s8756-3282\(01\)00641-x](https://doi.org/10.1016/s8756-3282(01)00641-x)

37. Braillon PM, Salle BL, Brunet J, Glorieux FH, Delmas PD, Meunier PJ. Dual energy x-ray absorptiometry measurement of bone mineral content in newborns: validation of the technique. *Pediatr Res*. 1992 Jul;32(1):77-80. <https://doi.org/10.1203/00006450-199207000-00015>

38. El Maghraoui A, Achemlal L, Bezza A. Monitoring of dual-energy X-ray absorptiometry measurement in clinical practice. *J Clin Densitom*. 2006 Jul-Sep;9(3):281-6. <https://doi.org/10.1016/j.jocd.2006.03.014>